

## Key Residues of Loop 3 in the Interaction with the Interface Residue at Position 14 in Triosephosphate Isomerase from *Trypanosoma brucei*<sup>†</sup>

Nallely Cabrera,<sup>‡</sup> Gloria Hernández-Alcántara,<sup>§</sup> Guillermo Mendoza-Hernández,<sup>△</sup> Armando Gómez-Puyou,<sup>‡</sup> and Ruy Perez-Montfort<sup>\*:‡</sup>

Departamento de Bioquímica, Instituto de Fisiología Celular, Universidad Nacional Autónoma de México, Apartado Postal 70242, 04510 México DF, Mexico, Laboratorio de Bioquímica-Genética, Instituto Nacional de Pediatría, 04530 México DF, Mexico, and Departamento de Bioquímica, Facultad de Medicina, Universidad Nacional Autónoma de México, 04510 México DF, Mexico

Received December 14, 2007; Revised Manuscript Received January 18, 2008

**ABSTRACT:** Cysteine 14 is an interface residue that is fundamental for the catalysis and stability of homodimeric triosephosphate isomerase from *Trypanosoma brucei* (TbTIM). Its side chain is surrounded by a deep pocket of 11 residues that are part of loop 3 of the adjacent monomer. Mutation of this residue to serine (producing single mutant C14S) yields a wild-type-like enzyme that is resistant to the action of sulfhydryl reagents methylmethane thiosulfonate (MMTS) and 5,5-dithiobis(2-nitrobenzoate) (DTNB). This mutant enzyme was a starting point for probing by cysteine scanning the role of four residues of loop 3 in the catalysis and stability of the enzyme. Considering that the conservative substitution of either serine or alanine with cysteine would minimally alter the structure and properties of the environment of the residue in position 14, we made double mutants C14S/A69C, C14S/S71C, C14S/A73C, and C14S/S79C. Three of these double mutants were similar in their kinetic parameters to wild-type TbTIM and the single mutant C14S, but double mutant C14S/A73C showed a greatly reduced  $k_{\text{cat}}$ . All enzymes had similar CD spectra, but all mutants had thermal stabilities lower than that of wild-type TbTIM. Intrinsic fluorescence was also similar for all enzymes, but the double mutants bound up to 50 times more 1-anilino-8-naphthalene sulfonate (ANS) and were susceptible to digestion with subtilisin. The double mutants were also susceptible to inactivation by sulfhydryl reagents. Double mutant C14S/S79C exhibited the highest sensitivity to MMTS and DTNB, bound a significant amount of ANS, and had the highest sensitivity to subtilisin. Thus, the residues at positions 73 and 79 are critical for the catalysis and stability of TbTIM, respectively.

The glycolytic enzyme triosephosphate isomerase (EC 5.3.1.1) from *Trypanosoma brucei* (TbTIM)<sup>1</sup> is a well-studied homodimer, which has an interface cysteine (C14) in its amino acid sequence. In trypanosomatidae, the enzyme is located in a specialized organelle called the glycosome; it catalyzes the interconversion between dihydroxyacetone phosphate and D-glyceraldehyde 3-phosphate. TbTIM has been proposed as a target for drug design by several research groups (1–4). TbTIM, like other TIMs, is active only as a dimer even though each monomer has all three amino acids that make up the active site. C14 is an interface residue that is surrounded by loop 3 of the adjoining subunit. The contacts established by these residues are essential for the enzymatic activity and stability of the protein. Previous experiments

by our group have shown that modifications like oxidation or derivatization of C14 with several sulfhydryl reagents such as methylmethane thiosulfonate (MMTS) and 5,5-dithiobis(2-nitrobenzoate) (DTNB) induce the abolition of catalysis by perturbing the interactions between C14 and the residues of loop 3 (5–9). This is caused by marked structural alterations that cause large changes in the intrinsic fluorescence of TbTIM (see Figure 5 of ref 6) and aggregation of the molecule (9).

The important role of C14 in maintaining the interactions that stabilize the interface of TbTIM was also confirmed by exhaustive mutagenesis of this amino acid (10); the results showed that only mutants C14T, C14A, C14P, C14V, and C14S had an activity that was practically identical to that of the wild-type enzyme (see Table 1 of ref 10). Mutants C14A and C14S, in particular, also had very similar stability to temperature, dilution, and other biophysical characteristics, when compared to the wild-type enzyme, but an important difference was that they were resistant to the derivatizing action of MMTS and DTNB (for example, see Figure 2A of ref 11). Since the amino acids serine and alanine have properties and sizes similar to those of cysteine and, when exchanged, are not expected to produce important structural and functional changes, we thought that the mutant TbTIMC14S, resistant to sulfhydryl reagents, could be used

<sup>†</sup> This work was supported in part by grants from CONACyT (49872) and from the Dirección General de Asuntos del Personal Académico, Universidad Nacional Autónoma de México (IN200507), to R.P.-M.

\* To whom correspondence should be addressed. Telephone: +52 (55) 5622 5657. Fax: +52 (55) 5622 5630. E-mail: ruy@ifc.unam.mx.

<sup>‡</sup> Universidad Nacional Autónoma de México.

<sup>§</sup> Instituto Nacional de Pediatría.

<sup>△</sup> Universidad Nacional Autónoma de México.

<sup>1</sup> Abbreviations: ANS, 1-anilino-8-naphthalene sulfonate; CD, circular dichroism; DTNB, 5,5-dithiobis(2-nitrobenzoate); MMTS, methylmethane thiosulfonate; PMSF, phenylmethanesulfonyl fluoride; SCM, spectral center of mass; TbTIM, triosephosphate isomerase from *Trypanosoma brucei*.

as a template for cysteine scanning of some of the residues of loop 3 that surround it. Loop 3, which includes residues 65–79 (12, 13), forms a deep pocket near the active site of the other subunit and has two serines and three alanines in its amino acid sequence; these are A67, A69, S71, A73, and S79. A67, which is at the beginning of loop 3, does not form part of the chain encircling the residue occupying position 14. It is 14.6 Å from that residue, and since no significant interaction would be likely between A67 and the residue at position 14, it was not included in this study. Thus, double mutants C14S/A69C, C14S/S71C, C14S/A73C, and C14S/S79C would be expected to be very similar in structure, and perhaps function, to the wild-type enzyme, but the newly introduced cysteines could be used to study the interactions of different regions of loop 3 surrounding the residue occupying position 14. Accordingly, we prepared the four double mutant enzymes and studied their kinetics, secondary structure, stability, fluorescent properties, and susceptibility to two sulfhydryl reagents. The data show that C79, which has no solvent accessible surface area and is closest to S14, is a critical residue whose interaction with the residue at position 14 is central to the stability of the enzyme. Our data suggest that the amino acid of loop 3 at position 79 is another hot spot and a good target for drug design against *T. brucei*.

## EXPERIMENTAL PROCEDURES

**Wild-Type TbTIM and Construction of the Mutants.** Wild-type TbTIM was expressed in *Escherichia coli* and purified as described by Borchert et al. (14). The construction, expression, purification, and properties of single mutant C14S have also been described previously (11). The four double mutants were constructed using the plasmid containing the sequence of the single mutant C14S as a template and introducing the second mutation with the polymerase chain reaction using the Expand High Fidelity PCR System (Boehringer). The mutagenic oligonucleotides were 5'GAACG CCATTGCAAGAGCGGTG3' forward (Fw) and 5'CAC-CGCTCTTCGAAATGGCGTTC3' reverse (Rv) for C14S/A69C, 5'TGCAAAGTGCAGTGCCTTACCG3' Fw and 5'CGGTGAAGGCACCGCACTTTGCA3' Rv for C14S/S71C, 5'AGAGCGGTTGCTTACCGGCGAA3' Fw and 5'TTCGCCGGTGAAGCAACCGCTC3' Rv for C14S/A73C, and 5'GGCGAAGTCTGCCTGCCCATCCTC3' Fw and 5'GAGGATGGGCAGGCAGACTTCGCC3' Rv for C14S/S79C. The external oligonucleotides were the T7 promoter and T7 terminator (Novagen). The mutations were introduced as follows: 25 cycles for 1 min at 94 °C, 1 min at 55 °C, and 1 min at 72 °C and the extension incubation for 10 min at 72 °C. The PCR products were cloned in the pET3a vector (Invitrogen) after digestion with *NdeI* and sequenced completely. The genes with the appropriate mutations were introduced by transformation into BL21(DE3)pLysS cells (Novagen).

For expression of the mutant proteins, cells were grown at 30 °C in Luria-Bertani medium supplemented with 100 µg/mL ampicillin. When cultures reached an  $A_{600}$  of 0.8–1.0, isopropyl β-D-thiogalactopyranoside, at a final concentration of 0.4 mM, was added. The growth of the cells was continued overnight at 30 °C. For the expression of wild-type TbTIM, growth occurred at 37 °C.

Cultures (1000 mL) were collected by centrifugation and suspended in 40 mL of cell lysis buffer (25 mM Mes/NaOH)

(pH 6.5), 1 mM dithiothreitol, 1 mM EDTA, and 0.2 mM phenylmethanesulfonyl fluoride (PMSF). The suspensions were sonicated, for five intervals of 40 s, and centrifuged at 15000 rpm (29000g) for 15 min. The pellet was resuspended in lysis buffer, which in addition had 200 mM NaCl, stirred gently on ice for 30 min, and centrifuged for 15 min at 15000 rpm (29000g). The purification of the mutants was also carried out following the methodology described by Borchert et al. (14).

After purification, all enzymes were dissolved in 100 mM triethanolamine, 10 mM EDTA, and 1 mM dithiothreitol (pH 8), precipitated with ammonium sulfate, and stored at 4 °C. Before use, the enzymes were dialyzed extensively against 100 mM triethanolamine and 10 mM EDTA (pH 7.4). Protein concentrations were determined from their absorbance at 280 nm using an extinction coefficient  $\epsilon$  of 34950 M<sup>-1</sup> cm<sup>-1</sup>, calculated according to the method of Pace et al. (15).

**Activity Assays.** Enzyme activities were determined at 25 °C, following the decrease in absorbance at 340 nm of a mixture (1 mL) that contained 100 mM triethanolamine, 10 mM EDTA (pH 7.4), 1 mM glyceraldehyde 3-phosphate, 0.2 mM NADH, and 0.9 unit of α-glycerol-3-phosphate dehydrogenase (20 µg/mL). The reaction was initiated by addition of the enzyme at the concentration indicated below. For the kinetic parameters, the measurements were made with glyceraldehyde 3-phosphate at concentrations that ranged between 0.06 and 2 mM. The concentration for all enzymes, except C14S/A73C, was 10 ng/mL (0.2 nM), and for C14S/A73C, it was 50 ng/mL (1 nM).  $K_m$  and  $k_{cat}$  were calculated from nonlinear regression plots using the Michaelis–Menten equation.

**Circular Dichroism Spectroscopy.** Circular dichroism (CD) spectra were obtained at 25 °C using an AVIV (Lakewood, NJ) 62 HDS spectropolarimeter. The quartz cells had path lengths of 0.1 cm for measurements in the far-UV region. For the determination of the spectra, solutions of the enzymes were equilibrated against a 25 mM phosphate buffer (pH 7.4) containing 20 mM NaCl. The samples were filtered through 0.45 µm membranes, and each enzyme had a final concentration of 250 µg/mL. Each spectrum was the average of five repetitive scans and was corrected by subtracting the average spectrum of the buffer. The molar ellipticity was calculated according to the equation

$$\theta = [\theta_{\text{obs}} (\text{degrees}) \times \text{MRW} \times 100] / (C \cdot l)$$

where  $\theta$  is the molar ellipticity in degrees,  $\theta_{\text{obs}}$  is the observed ellipticity, MRW is the mean residue weight,  $C$  is the protein concentration in milligrams per milliliter, and  $l$  is the path length of light in the cell (16).

**Thermal Unfolding.** Thermal denaturation of the enzymes was performed by recording the protein ellipticity at 222 nm between 20 and 70 °C, increasing the temperature of the samples at a rate of 1 °C/2.5 min. The enzymes (400 µg/mL or 350 µM) were dialyzed before the experiments against a 20 mM MOPS buffer (pH 7.0) containing 1 mM EDTA, 1 mM dithiothreitol, and 1 mM azide. The apparent fraction of denatured subunits,  $f_D$ , was calculated using the equation

$$f_D = (y_N - y) / (y_N - y_D)$$

where  $y_N$  and  $y_D$  are the ellipticity values characteristic of the native and unfolded subunits, respectively. These parameters were linear extrapolations from the initial and final portions of the curve of  $y$  versus temperature.

**Fluorescence Measurements and 1-Anilino-8-naphthalene Sulfonate (ANS) Binding.** The emission fluorescence spectra of all enzymes were recorded between 300 and 500 nm at excitation wavelengths of 280 and 295 nm with a Perkin-Elmer LS55 spectrofluorometer. The protein concentration was 50  $\mu\text{g}/\text{mL}$  in 100 mM triethanolamine and 10 mM EDTA (pH 7.4). The spectrum of the buffer was subtracted from the experimental spectrum, and the spectral center of mass (SCM) was calculated with the equation

$$\text{SCM} = \frac{\sum \lambda I(\lambda)}{\sum I(\lambda)}$$

where  $I(\lambda)$  is the fluorescence intensity at wavelength  $\lambda$ .

ANS fluorescence was measured with an excitation wavelength of 360 nm (4.0 nm bandwidth) and read in the 400–600 nm emission range. Saturation conditions at 25  $\mu\text{M}$  ANS were used; 200  $\mu\text{g}$  of each enzyme was incubated at 25  $^{\circ}\text{C}$  in 100 mM triethanolamine and 10 mM EDTA (pH 7.4) for 15 min with 25  $\mu\text{M}$  ANS, and the corresponding blanks were subtracted from the spectra of the samples. The results are expressed as arbitrary units of fluorescence for each enzyme.

**Effect of MMTS and DTNB.** The enzymes were incubated at the following concentrations: TbTIM at 10  $\mu\text{g}/\text{mL}$ , C14S and C14S/A69C at 150  $\mu\text{g}/\text{mL}$ , and C14S/S71C, C14S/A73C, and C14S/S79C at 300  $\mu\text{g}/\text{mL}$ . The mutant enzymes were used at higher concentrations because they spontaneously lost activity at the lower concentration. [The same results were obtained when TbTIM, C14S, and C14S/A69C were assayed at 300  $\mu\text{g}/\text{mL}$  (data not shown).] All enzymes were incubated at 25  $^{\circ}\text{C}$  in 100 mM triethanolamine and 10 mM EDTA (pH 7.4) for 2 h in the presence of the indicated concentrations of MMTS or DTNB. The activity was measured after the incubation using 5 ng of enzyme, except for C14S/A73C, for which 10 ng was necessary, and addition to the reaction mixture. The results are expressed as the percentage of the activity of the controls, where 100% was the activity of enzymes incubated without the sulfhydryl reagents.

**Number of Cysteines Derivatized by DTNB as a Function of Time.** Wild-type TbTIM and the mutants (300  $\mu\text{g}$ ) were incubated at 25  $^{\circ}\text{C}$  in 1 mL of a mixture that contained 100 mM triethanolamine, 10 mM EDTA, and 3 mM DTNB (pH 7.4) for 20 min. The absorbance at 412 nm was recorded immediately after the enzymes were added. The blank (with no enzyme) exhibited a slight increase in absorbance at 412 nm; this was subtracted from the experimental values. The number of derivatized cysteines ( $N$ ) was calculated with the equation

$$N = (A_{412}/\epsilon)/$$

(protein concentration in milligrams/MW of the protein)

where  $A$  is the absorbance and  $\epsilon$  the extinction coefficient of nitrobenzoic acid.

**Proteolytic Digestion, Electrophoresis, and  $\text{NH}_2$ -Terminal Analysis of Electroblooded Fragments.** The double mutants C14S/S71C, C14S/A73C, and C14S/S79C were incubated at a concentration of 1  $\text{mg}/\text{mL}$  with subtilisin Carlsberg at the indicated molar ratios in 100 mM triethanolamine and 10 mM EDTA (pH 7.4) at 30  $^{\circ}\text{C}$  for the indicated times. Proteolysis was arrested by the addition of PMSF (3 mM final concentration). The digested TIMs were analyzed via SDS-PAGE in gels containing 16% acrylamide following

Table 1: Kinetic Constants of Wild-Type TbTIM and the Indicated Mutants<sup>a</sup>

| enzyme    | $K_m$ ( $\times 10^{-4}$ M) | $k_{\text{cat}}$ ( $\text{s}^{-1}$ ) | $k_{\text{cat}}/K_m$ ( $\times 10^6$ $\text{s}^{-1}$ $\text{M}^{-1}$ ) |
|-----------|-----------------------------|--------------------------------------|--|
| wild type | $3.8 \pm 0.4$               | $4183 \pm 55$                        | 11.0   |
| C14S      | $5.0 \pm 0.6$               | $5133 \pm 170$                       | 10.3   |
| C14S/A69C | $7.5 \pm 0.4$               | $2600 \pm 142$                       | 3.5  |
| C14S/S71C | $3.5 \pm 0.3$               | $3200 \pm 112$                       | 9.1  |
| C14S/A73C | $1.4 \pm 0.3$               | $483 \pm 28$                         | 3.5  |
| C14S/S79C | $4.8 \pm 0.5$               | $2967 \pm 137$                       | 6.2  |

<sup>a</sup> The measurements were made with glyceraldehyde 3-phosphate at concentrations between 0.06 and 2 mM. The reaction was started by addition of the enzyme. A concentration of 5  $\text{ng}/\text{mL}$  was used with all enzymes, except C14S/A73C, for which a concentration of 10  $\text{ng}/\text{mL}$  was employed.  $K_m$  and  $k_{\text{cat}}$  were calculated from nonlinear regression plots using the Michaelis–Menten equation. The data are the average of at least two independent determinations.

the method of Schagger and von Jagow (17). The gels were stained with Coomassie Brilliant Blue G. The fragments of the digested TIMs were electroblotted from the stained gels onto polyvinylidene difluorobenzene membranes (Problott). The semi dry transfer was performed for 2 h at room temperature using as a negative buffer 39.4 g/L aminocaproic acid (pH 8.5) with 0.05% SDS and as a positive buffer 8.2 g/L Tris, 9 g/L Tricine, and 20% methanol. The transferred proteins were stained with Coomassie Brilliant Blue G in 50% methanol. The N-terminal sequence was determined by automated Edman degradation on a gas-phase protein sequencer (LF 30000 Beckman Instruments) equipped with an online Beckman System Gold high-performance liquid chromatography (HPLC) system. The HPLC equipment had a model 126 pump and a diode array detector set at 268 and 293 nm for signal and reference, respectively. The HPLC column was a Beckman Spherogel Micro PTH column (2 mm  $\times$  150 mm). Standard Beckman sequencing reagents were used. To establish the cleavage sites unequivocally, the sequenced bands were submitted to at least 10 Edman degradation cycles. In all cycles in which more than one amino acid was obtained, the yield of each identified amino acid was considered for the determination of the sequence of each fragment.

## RESULTS

**Kinetics of Wild-Type TbTIM, the Single C14S Mutant, and the C14S/A69C, C14S/S71C, C14S/A73C, and C14S/S79C Double Mutants.** The steady state kinetics of the wild type, the single C14S mutant, and the four double mutants were determined in the direction of glyceraldehyde 3-phosphate to dihydroxyacetone phosphate. The  $K_m$  and  $k_{\text{cat}}$  values of the wild type, the single C14S mutant, and the four double mutants are listed in Table 1. As previously reported (10), the wild type and the single mutant exhibited similar kinetic constants; the  $K_m$  and the  $k_{\text{cat}}$  of the double mutant C14S/S71C mutant were in the same range. The other double mutants exhibited lower  $k_{\text{cat}}/K_m$  values, mainly as consequence of a lower  $k_{\text{cat}}$ ; the latter decrease was particularly noticeable in the C14S/A73C double mutant.

**Spectroscopy and Thermal Stability of Wild-Type TbTIM and Mutants.** The circular dichroism spectra of wild-type TbTIM and the mutants were recorded between 190 and 260 nm at 25  $^{\circ}\text{C}$  (Figure 1). All spectra were similar to that of wild-type TbTIM, indicating that the different mutations did not cause gross alterations of secondary structure. Thermal

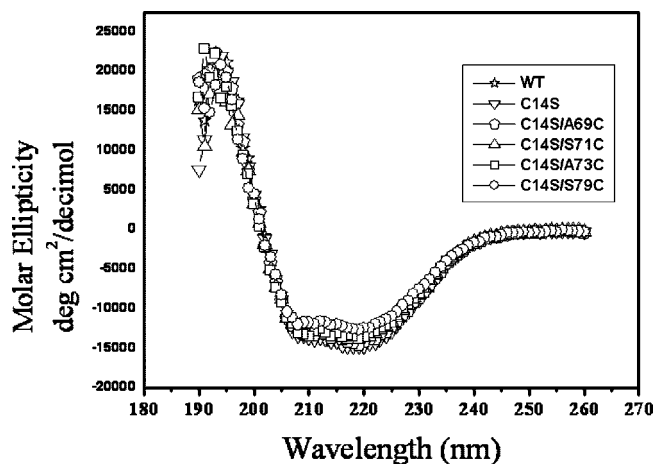


FIGURE 1: CD spectra of wild-type TbTIM and the indicated mutants. The spectra of the indicated enzymes were recorded at protein concentrations of 250  $\mu\text{g}/\text{mL}$  in 25 mM phosphate buffer (pH 7.4) containing 20 mM NaCl.

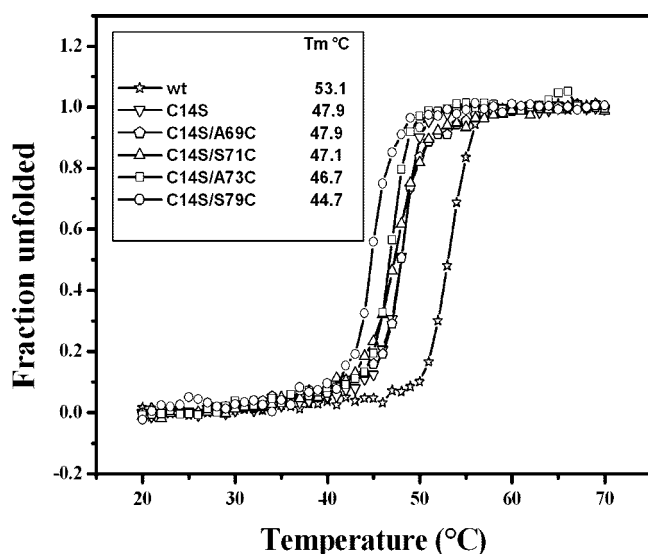


FIGURE 2: Melting curves of wild-type TbTIM and the indicated mutants. The changes in molar ellipticity induced by the progressive increase in temperature were followed at 222 nm. The inset shows the  $T_m$  values of the indicated enzymes.

denaturation experiments were carried out at an enzyme concentration of 350  $\mu\text{g}/\text{mL}$  by recording the signal at 222 nm at temperatures that ranged from 20 to 70 °C (Figure 2). The results indicated that, in all cases, the loss of secondary structure occurred in a two-state process; however, there were differences in the apparent  $T_m$  of the various enzymes. The  $T_m$  of the single C14S mutant was 5.2 °C lower than that of the wild type, which was 53.1 °C, highlighting the importance of C14 in the thermal stability of the enzyme. Using the data of the single mutant as a reference for the impact of the second mutation, it is noteworthy that with the exception of C14S/S79C, the  $T_m$  values of other double mutants differed by less than 1.2 °C from that of the single mutant. In contrast, the  $T_m$  of the C14S/S79C double mutant was 3.2 °C lower than that of the single mutant, suggesting that residue 79 is also central to the thermal stability of the enzyme.

**Intrinsic Fluorescence and ANS Binding.** To gain insight into the effect of the second mutation on the gross structure of the enzymes, the intrinsic fluorescence spectra of the

Table 2: Spectral Centers of Mass and Percentages of Intrinsic Fluorescence of Wild-Type TbTIM and the Indicated Mutants<sup>a</sup>

| enzyme    | SCM at 280 nm | % FI at 280 nm |
|-----------|---------------|----------------|
| wild type | 344           | 100            |
| C14S      | 344           | 109            |
| C14S/A69C | 344           | 103            |
| C14S/S71C | 348           | 106            |
| C14S/A73C | 348           | 100            |
| C14S/S79C | 349           | 123            |

<sup>a</sup> The intrinsic fluorescence spectra of 50  $\mu\text{g}$  of the indicated enzymes were obtained at an excitation wavelength of 280 nm. The spectral center of mass (SCM) and relative fluorescence intensity (FI) were calculated from the spectra. The fluorescence intensity of the wild-type enzyme at the wavelength of maximal emission was considered 100%.

Table 3: ANS Fluorescence (in arbitrary units) of Wild-Type TbTIM and the Indicated Mutants<sup>a</sup>

| enzyme    | ANS fluorescence intensity |
|-----------|----------------------------|
| wild type | 0                          |
| C14S      | 14.6                       |
| C14S/A69C | 57.0                       |
| C14S/S71C | 195.9                      |
| C14S/A73C | 278.0                      |
| C14S/S79C | 732.3                      |

<sup>a</sup> ANS (25  $\mu\text{M}$ ) was added to each enzyme. The fluorescence intensity was recorded between 400 and 600 nm (excitation wavelength of 360 nm and maximum emission wavelength of 480 nm). The concentration of the protein was 267  $\mu\text{g}/\text{mL}$ .

various enzymes were determined after excitation at 280 nm. From the data, the spectral center of mass (SCM) and the intensity of fluorescence at that wavelength were calculated (Table 2). The spectra of the wild type, the single mutant, and C14S/A69C exhibited the same SCM, but the fluorescence intensities of the latter two mutants were slightly higher than that of the wild type. The other double mutants exhibited a SCM 4 nm higher; however, it is noteworthy that among the enzymes that were studied, the C14S/S79C double mutant, besides showing a red shift with respect to the single C14S mutant, also exhibited the highest fluorescence intensity.

Using the C14S single mutant as a reference for the second mutation, the CD and fluorescence data indicated that the S79C mutation induces significant changes in thermostability and in the environment of aromatic residues. To gain further insight into this phenomenon, we explored if the mutation also affects the exposure of hydrophobic residues to the solvent. To this end, we measured the fluorescence of ANS when it was incubated with the various enzymes; this is because it is well-established that the fluorescence of ANS increases when it binds to hydrophobic surfaces. In the wild type, no fluorescence of ANS was observed and the single C14S mutant exhibited a very small fluorescence signal. The ANS fluorescence in the double mutants was significantly higher (Table 3); the magnitude of ANS binding in the double mutants was as follows: C14S/S79C > C14S/A73C > C14S/S71C > C14S/A69C. However, it is noteworthy that the level of ANS fluorescence in the C14S/S79C mutant was 50 times higher than in the single C14S mutant. This is in consonance with the CD data and intrinsic fluorescence of the enzymes that show that the most drastic differences with the single mutant were observed when S79 of the single mutant was replaced with cysteine.

**Proteolysis of the Enzymes.** The sensitivity of the enzymes to external probes was also examined by measuring their susceptibility to the proteolytic enzyme subtilisin. As reported

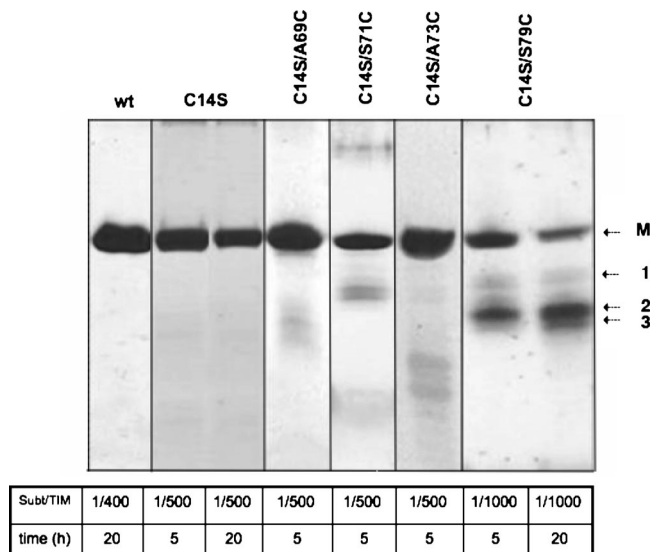


FIGURE 3: SDS-PAGE analysis of the hydrolysis of wild-type TbTIM and the indicated mutants with subtilisin. The enzymes were incubated at 30 °C with subtilisin at different times and different subtilisin:enzyme ratios. At the indicated time, the reactions were arrested with 3 mM PMSF. The arrows show the TbTIM monomer (M) and three fragments of C14S/S79C that were sequenced. The amino-terminal amino acids for fragment 1 were S71 and A73, for fragment 2 S71, G72, and A73, and for fragment 3 S71, A73, K84, and G87.

elsewhere, native wild-type TbTIM is quite resistant to the action of subtilisin (18); indeed, the incubation of four TbTIM molecules per subtilisin molecule did not produce a noticeable amount of proteolytic fragments after incubation for 20 h (Figure 3). The single mutant showed a similar resistance. In contrast, in all the double mutants, proteolysis was clearly apparent; however, the extent of proteolysis of the C14S/S79C double mutant was significantly higher, even at ratios of one subtilisin per 1000 enzymes (Figure 3). Proteolysis in the C14S/S79C double mutant was accompanied by the appearance of two main protein bands that had a molecular mass of 16 kDa. These were subjected to Edman degradation to ascertain the cleavage sites. The data showed that the enzyme was cleaved in the peptide bonds between K70 and S71, S71 and G72, and G72 and A73; additional cleavage products that started with K84 and G87 were also observed (see Figure 3). It is noted that the double mutants C14S/S71C and C14S/A73C were also cleaved at a ratio of 500 enzymes per subtilisin in the same peptide bonds; albeit, the extent of cleavage was much lower than in C14S/S79C (data not shown).

Taken together, the data showed that there are drastic and noteworthy differences in the action of subtilisin on wild-type TbTIM and the double mutants. At ratios of four wild-type TbTIM molecules per subtilisin, the main cleavage products were between T130 and N131 and between Q181 and Q182 (18). In contrast, in the C14S/S79C double mutant, significant proteolysis was observed at ratio of 1000 enzymes per subtilisin, and the main cleavage sites were localized in the span of S71–A73. Since the latter amino acids form part of loop 3, the data indicate that the replacement of S79 with cysteine increases the level of exposure of this portion of loop 3 to subtilisin. The other double mutants were less sensitive to proteolysis; nonetheless, fragments that began in the same amino acid regions were observed.

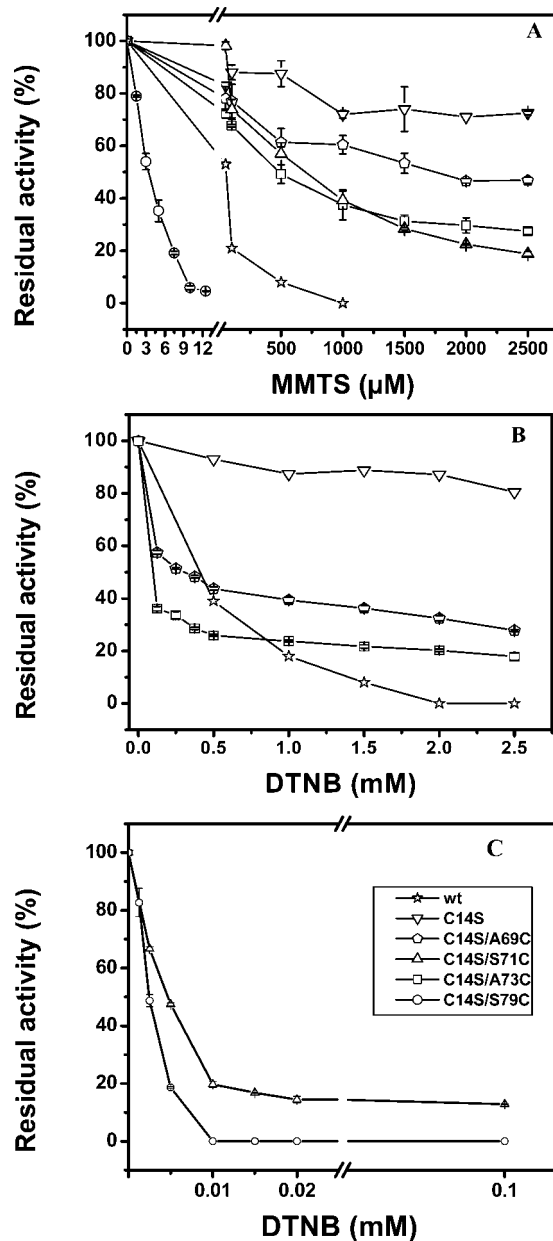


FIGURE 4: Effect of MMTS (A) and DTNB (B and C) on the activity of wild-type TbTIM and the indicated mutants. The enzymes were incubated as described in Experimental Procedures. The results are expressed as the percentage of the activity of the controls in which 100% was the activity of enzymes incubated without the sulfhydryl reagents. After incubation for 2 h, the activity was measured with a concentration 5 ng/mL, except for C14S/A73C, for which 10 ng/mL was used.

*Susceptibility of Wild-Type TbTIM and the Mutants to Thiol Reagents.* The preceding experiments indicated that the introduction of a second mutation into loop 3 of the C14S single mutant increased the exposure to solvent of the region of loop 3 that spans S71–A73. Thus, it was considered relevant to determine the accessibility of the cysteines, which were introduced in loop 3, to external probes that are specific for the SH groups. Toward this end, the effect of different concentrations of the sulfhydryl reagents MMTS and DTNB on the activity of the various enzymes was determined. In confirmation of previous data (6), we observed that the wild type is 50% inhibited by ~100  $\mu$ M MMTS and that complete inhibition is achieved with 500  $\mu$ M (Figure 4). Of relevance to the current experiments is the fact that in the single C14S

Table 4: Number of Cysteines Derivatized per Dimer of Wild-Type TbTIM and the Indicated Mutants by DTNB in 20 min<sup>a</sup>

| enzyme    | no. of cysteines derivatized per dimer |
|-----------|--|
| wild type | 0.8 ± 0.1                              |
| C14S      | 0.0                                    |
| C14S/A69C | 0.8 ± 0.1                              |
| C14S/S71C | 1.4 ± 0.4                              |
| C14S/A73C | 2.3 ± 0.2                              |
| C14S/S79C | 6.3 ± 0.1                              |

<sup>a</sup> The concentration of all proteins was 300 μg/mL (22.4 μM dimer), and they were incubated at 25 °C in 1 mL of a mixture that contained 100 nM triethanolamine, 10 mM EDTA (pH 7.4), and 3.3 mM DTNB. The absorbance at 412 nm was recorded immediately after enzymes were added. The blank (without enzymes) exhibited a slight increase in absorbance at 412 nm; this was subtracted from the experimental values.

mutant, millimolar concentrations of MMTS induced only a relatively small loss of activity. Therefore, the latter enzyme provided a good point of reference for exploring the effect of sulfhydryl reagents on the double mutants, since the results would illustrate the impact of derivatizing the cysteines that were introduced into loop 3 of the double mutants. The activity of all the double mutants was inhibited by MMTS; albeit, when compared to the wild type, the C14S/A69C, C14S/A73C, and C14S/S71C double mutants were more resistant to MMTS action (Figure 4A). Remarkably, the C14S/S79C double mutant was highly susceptible to MMTS action; i.e., its activity was inhibited by 50% with 3 μM MMTS (Figure 4A).

The susceptibility of the enzymes to DTNB was also determined. In agreement with previous data, it was observed that the activity of the wild type was inhibited by DTNB (9) and that the C14S single mutant was essentially insensitive to DTNB. Thus, the effect of DTNB on the activity of the double mutants should be due to derivatization of the introduced cysteines. The results of these experiments showed that all the double mutants were more sensitive to DTNB than the wild type (Figure 4B,C). However, the susceptibility of the C14S/S71C and C14S/S79C double mutants was much higher; indeed, 10 μM DTNB induced a very strong inhibition of both enzymes.

The latter results correlate with the number of cysteines that are derivatized by DTNB. In the experiments outlined in Table 4, the various enzymes were allowed to react with 3.3 mM DTNB for 20 min at which time the number of cysteines was quantified from the molar absorption of thionitrobenzoic acid that was formed. In the C14S single mutant, no reaction with DTNB was observed, and in the wild type and the C14S/A69C and C14S/S71C double mutants, close to one cysteine per dimer was derivatized. In the double mutant C14S/A73C, two cysteines per dimer were derivatized, whereas in the C14S/S79C double mutant, all six cysteines of the dimer reacted with DTNB.

## DISCUSSION

It has been shown that the integrity of C14 is central to the stability of TIM dimers (10). This is a consequence of its critical position in the dimer interface; indeed, as shown in Figure 5, the side chain of C14 is enclosed by residues of loop 3 of the adjoining subunit. The purpose of this work was to determine the contribution of the residues of loop 3 that are close to residue 14 to the stability and catalysis of the TIM dimer. Because we also wanted to ascertain how

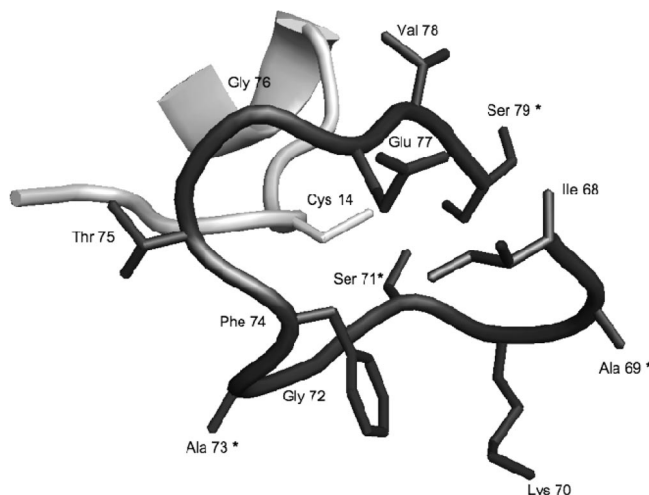


FIGURE 5: Close-up view of the relative position of C14 of one subunit (light gray) with residues of loop 3 from the other subunit (dark gray). The  $\alpha$ -carbon traces of the two subunits are shown as ribbons and tubes, and the side chains of C14 and 12 residues of loop 3 of the other subunit are shown as sticks. The residues of loop 3 that were mutated are marked with an asterisk. The three-dimensional coordinates are from PDB entry 5TIM.

the perturbation of such residues affects the characteristics of the dimer, the C14S mutant of TbTIM was the enzyme into which the second mutations were introduced. It is important to note that although the  $T_m$  of the C14S mutant was lower than that of the wild type, its catalytic constants, intrinsic fluorescence, CD spectra, and capacity to bind ANS were markedly similar to those of the wild type. Moreover, since the single mutant lacks cysteine at position 14, it was essentially insensitive to thiol reagents, and thus, the evaluation of the effect of thiol reagents on mutants in which cysteines were placed at various positions of loop 3 was straightforward. As shown in this work, the introduction of the second mutation did not have an important effect on catalysis, except in C14S/A73C by which a substantial decrease in  $k_{cat}$  was observed.

However, a comparison of some of the properties of the double mutants with those of the wild type and the C14S single mutant showed that the replacement in the single mutant of residues A69, S71, and A73 with cysteine induced changes in their capacity to bind ANS and made the enzymes more accessible to subtilisin action. However, these alterations were rather minor in comparison to those observed in the C14S/S79C double mutant. Furthermore, the latter mutant had a  $T_m$  3 °C lower than that of the single mutant. Thus, the overall data indicate that among the residues tested, residue 79 plays a central role in the overall structure and stability of the enzyme.

In this context, it is relevant that in a crystal structure of wild-type TbTIM (12), the solvent accessible surface areas of A69, S71, and A73 are 34, 40.9, and 45.9 Å<sup>2</sup>, respectively; in contrast, S79 is completely buried. In the wild type, S79 is less than 4 Å from C14 of the other subunit and from residues 68, 70–72, 78, 80, 82, and 83 of the same subunit (see Figure 5; residues 80, 82, and 83 are not shown). Thus, its tight packing within loop 3 and C14 of the other subunit explains why the substitution of serine for the less polar and larger (by 19.5 Å<sup>3</sup>) cysteine exerts such drastic changes.

Along this line, it is relevant that in the C14S/S79C double mutant, subtilisin brought about cleavage between residues

K70 and S71, and between S71 and G72 of loop 3. These residues are not cleaved in the single mutant; thus, the S79C mutation brought about conformational changes in loop 3 that made it prone to proteolytic cleavage. It is noted that in the crystal structure of wild-type TbTIM, the residues that are at the main cleavage sites of subtilisin in the C14S/S79C mutant are between K70 and S71 and between S71 and G72. S71 and G72 have buried surface areas of 20 and 40 Å<sup>2</sup>, respectively. Glycine has a total surface area of 75 Å<sup>2</sup>; thus, more than half of its surface is buried in the native structure, yet in C14S/S79C, the peptide bond between S71 and G72 is readily accessible to subtilisin.

In all likelihood, the latter conformational changes of the C14S/S79C mutant account for the high sensitivity of the mutant to MMTS; indeed, it is remarkable that concentrations as low as 10 μM induce almost full abolition of catalysis. Therefore, the data indicate that the integrity of S79 is central in the overall conformation of loop 3, and that this has a strong bearing on the stability of the TIM dimer. S79 is a highly conserved residue; among 723 TIM aligned amino acid sequences, 86% have serine at position 79 and 7% have alanine, which has dimensions and polarity similar to those of serine. Therefore, the sequence analysis and the data of this work highlight the importance of S79 in the stability of TIM. An alanine in position 73 is present in 90% of the sequences that were analyzed. However, its substitution for cysteine did not affect to a large extent the stability of the dimer; albeit, it induced a marked decrease in  $k_{cat}$ . It would thus appear that A73 is mostly related to the catalytic events, whereas the role of S79 is to exert a strong effect on the stability of the enzyme.

In summary, the data presented here show that among the residues that constitute the portion of the interface formed by loop 3 and residue 14 of the other monomer, the amino acid at position 79 is fundamental in maintaining enzyme stability. In this regard, and before closing, we note that for some years we have been interested in discovering low-molecular weight compounds that induce abolition of catalysis in enzymes from pathogenic parasites. Because of the high level of conservation in the active site, we hypothesized that the interface of the TIM dimers could be targeted for the discovery of such agents (6). Some of the molecules that exert this action have been described previously (19–22). In consonance with the hypothesis, the findings of this work show that rather subtle alterations of the amino acids that form the interface of the TIM dimer, in particular the residue at position 79, have profound effects on the stability of the dimer, and thus, it could be expected that agents that perturb the portion of the dimer interface could have detrimental effects on the overall properties of the enzyme.

#### ACKNOWLEDGMENT

We thank Dr. P. A. M. Michels (Research Unit for Tropical Diseases, ICP-TROP, Brussels, Belgium) for the TbTIM gene. The technical assistance of Dr. Laura Ongay Larios, María Guadalupe Codiz Huerta, and Minerva Mora Cabrera of the Unidad de Biología Molecular at the Instituto de Fisiología Celular, Universidad Nacional Autónoma de México, is also gratefully acknowledged.

#### REFERENCES

- Verlinde, C. L., Merritt, E. A., Van den Akker, F., Kim, H., Feil, I., Delboni, L. F., Mande, S. C., Sarfaty, S., Petra, P. H., and Hol, W. G. (1994) Protein crystallography and infectious diseases. *Protein Sci.* 3, 1670–1686.
- Gao, X.-G., Maldonado, E., Pérez-Montfort, R., Garza-Ramos, G., Tuena de Gómez-Puyou, M., Gómez-Puyou, A., and Rodríguez-Romero, A. (1999) Crystal Structure of triosephosphate isomerase from *Trypanosoma cruzi* in hexane. *Proc. Natl. Acad. Sci. U.S.A.* 96, 10062–10067.
- Singh, S. K., Maithal, K., Balam, H., and Balam, P. (2001) Synthetic peptides as inactivators of multimeric enzymes: Inhibition of *Plasmodium falciparum* triosephosphate isomerase by interface peptides. *FEBS Lett.* 501, 19–23.
- Rodríguez-Romero, A., Hernández-Santoyo, A., del Pozo Yauner, L., Kornhauser, A., and Fernández-Velasco, D. A. (2002) Structure and inactivation of triosephosphate isomerase from *Entamoeba histolytica*. *J. Mol. Biol.* 322, 669–675.
- Zubillaga, R. A., Pérez-Montfort, R., and Gómez-Puyou, A. (1994) Differential inactivation of rabbit and yeast triose phosphate isomerase. Effect of oxidations produced by chloramine-T. *Arch. Biochem. Biophys.* 313, 328–336.
- Gómez-Puyou, A., Saavedra-Lira, E., Becker, I., Zubillaga, R. A., Rojo-Domínguez, A., and Pérez-Montfort, R. (1995) Using evolutionary changes to achieve species specific inhibition of enzyme action. Studies with triosephosphate isomerase. *Chem. Biol.* 2, 847–855.
- Garza-Ramos, G., Pérez-Montfort, R., Rojo-Domínguez, A., Tuena de Gómez-Puyou, M., and Gómez-Puyou, A. (1996) Species specific inhibition of homologous enzymes by modification of nonconserved amino acids. The cysteines of triosephosphate isomerase. *Eur. J. Biochem.* 241, 114–120.
- Maldonado, E., Moreno, A., Panneerselvam, K., Ostoa-Saloma, P., Garza-Ramos, G., Soriano-García, M., Pérez-Montfort, R., Tuena de Gómez-Puyou, M., and Gómez-Puyou, A. (1997) Crystallization and preliminary X-ray analysis of triosephosphate isomerase from *Trypanosoma cruzi*. *Protein Pept. Lett.* 4, 139–144.
- Garza-Ramos, G., Cabrera, N., Saavedra-Lira, E., Tuena de Gómez-Puyou, M., Ostoa-Saloma, P., Pérez-Montfort, R., and Gómez-Puyou, A. (1998) Sulfhydryl reagent susceptibility in proteins with high sequence similarity-triosephosphate isomerase from *Trypanosoma brucei*, *Trypanosoma cruzi* and *Leishmania mexicana*. *Eur. J. Biochem.* 253, 684–691.
- Hernández-Alcántara, G., Garza-Ramos, G., Mendoza-Hernández, G., Gómez-Puyou, A., and Pérez-Montfort, R. (2002) Catalysis and stability of triosephosphate isomerase from *Trypanosoma brucei* with different residues at position 14 of the dimer interface. Characterization of a catalytically competent monomeric enzyme. *Biochemistry* 41, 4230–4238.
- Pérez-Montfort, R., Garza-Ramos, G., Hernández-Alcántara, G., Reyes-Vivas, H., Gao, X. G., Maldonado, E., Tuena de Gómez-Puyou, M., and Gómez-Puyou, A. (1999) Derivatization of the interface cysteine of triosephosphate isomerase from *Trypanosoma brucei* and *Trypanosoma cruzi* as a probe of the interrelationship between the catalytic sites and the dimer interface. *Biochemistry* 38, 4114–4120.
- Wierenga, R. K., Noble, M. E. M., Vriend, G., Nauche, S., and Hol, W. G. J. (1991) Refined 1.83 Å structure of trypanosomal triosephosphate isomerase crystallized in the presence of 2.4 Å ammonium sulphate: A comparison with the structure of the trypanosomal triosephosphate isomerase-glycerol-3-phosphate complex. *J. Mol. Biol.* 220, 995–1015.
- Maldonado, E., Soriano-García, M., Moreno, A., Cabrera, N., Garza-Ramos, G., Tuena de Gómez-Puyou, M., Gómez-Puyou, A., and Pérez-Montfort, R. (1998) Differences in the intersubunit contacts in triosephosphate isomerase from two closely related pathogenic trypanosomes. *J. Mol. Biol.* 283, 193–203.
- Borchert, T. V., Pratt, K., Zeelen, J. P., Callens, M., Noble, M. E., Opperdoes, F. R., Michels, P. A., and Wierenga, R. K. (1993) Overexpression of trypanosomal triosephosphate isomerase in *Escherichia coli* and characterization of a dimer-interface mutant. *Eur. J. Biochem.* 211, 703–710.
- Pace, C. N., Vajdos, F., Fee, L., Grisley, G., and Gray, T. (1995) How to measure and predict the molar absorption coefficient of a protein. *Protein Sci.* 4, 2411–2423.
- Schmid, F. X. (1989) Spectral methods of characterizing protein conformation and conformational changes, in *Protein Structure*.

- A Practical Approach* (Creighton, T. E., Ed.) pp 251–283, IRL Press at Oxford University Press, Oxford, U.K.
17. Schägger, H., and von Jagow, G. (1987) Tricine-sodium dodecyl sulfate polyacrylamide gel electrophoresis for the separation of proteins in the range of 1 to 100 kDa. *Anal. Biochem.* *166*, 368–379.
  18. Reyes-Vivas, H., Martínez-Martínez, E., Mendoza-Hernández, G., López-Velázquez, G., Pérez-Montfort, R., Tuena de Gómez-Puyou, M., and Gómez-Puyou, A. (2002) Susceptibility to proteolysis of triosephosphate isomerase from two pathogenic parasites: Characterization of an enzyme with an intact and a nicked monomer. *Proteins* *48*, 580–590.
  19. Tellez-Valencia, A., Avila-Rios, S., Pérez-Montfort, R., Rodríguez-Romero, A., Tuena de Gómez-Puyou, M., López-Calahorra, F., and Gómez-Puyou, A. (2002) Highly specific inactivation of triosephosphate isomerase from *Trypanosoma cruzi* by agents that act on the dimer interface. *Biochem. Biophys. Res. Commun.* *295*, 958–963.
  20. Téllez-Valencia, A., Olivares-Illana, V., Hernández-Santoyo, A., Pérez-Montfort, R., Costas, M., Rodríguez-Romero, A., López-Calahorra, F., Tuena de Gómez-Puyou, M., and Gómez-Puyou, A. (2004) Inactivation of triosephosphate isomerase from *Trypanosoma cruzi* by an agent that perturbs its dimer interface. *J. Mol. Biol.* *341*, 1355–1365.
  21. Olivares-Illana, V., Perez-Montfort, R., López-Calahorra, F., Costas, M., Rodriguez-Romero, A., Tuena de Gómez-Puyou, M., and Gómez-Puyou, A. (2006) Structural differences in TIM from different species and the discovery of a multi-trypanosomatid inhibitor. *Biochemistry* *45*, 2556–2560.
  22. Olivares -Illana, V., Rodríguez-Romero, A., Becker, I., Berzunza, M., García, J., Pérez-Montfort, R., Cabrera, N., López-Calahorra, F., Tuena de Gómez-Puyou, M., and Gómez-Puyou, A. (2007) Perturbation of the dimer interface of triosephosphate isomerase and its effect on *Trypanosoma cruzi*. *PLoS Neglected Trop. Dis.* *1*, e01.

BI702439R